Differential coupling of visual cortex with default network or frontal-parietal network based on goals

Supplementary Material

James Z. Chadick and Adam Gazzaley

SUPPLEMENTARY METHODS

Participants: Functional and high-resolution anatomical MRI images were obtained from 22 healthy young participants (ages: 18-34, mean: 23.7) while performing the task described below. Participants were recruited and compensated monetarily as per the UCSF Committee on Human Research (CHR) approval. All participants had normal or corrected-to-normal vision and were taking no psychotropic medications. One participant was excluded from all analysis due to excessive motion artifacts (> 3 mm) within the scanner.

Experimental Design. The experimental paradigm was comprised of five similar tasks in a delayed-recognition working memory (WM) task design (Fig. 1), similar to previously published work [1]. Each task consisted of the same basic temporal sequence with only the instructions differing across tasks. All tasks involved viewing two images (Stim1, Stim2), each displayed for 800 ms (with a 400 ms inter-stimulus interval [ISI]) followed by a 8 second period (Delay) in which the images were to be remembered and mentally rehearsed. After the delay, a third image appeared (Probe) for 1000 sec. The participant was instructed to respond with a button press (as quickly as possible without sacrificing accuracy) whether or not the Probe image matched either of the previous two images (Stim1 or Stim2). This was followed by an inter-trial interval (ITI) lasting 9 seconds.

For three of the five tasks, the Stim1 and Stim2 images were comprised of both a scene and a face superimposed upon each other. Participants were instructed to focus their attention on and remember either the face or the scene, while ignoring the other. In the face memory-overlap task (FM-O), the faces were remembered while the scenes were ignored, and vice versa in the scene memory-overlap task (SM-O). When the Probe image appeared, it was composed of an isolated face in the FM-O task, and an

isolated scene in the SM-O task. For the passive view (PV-O) task, participants were instructed to view the overlapped images without trying to remember them, after which they responded to an arrow direction with a button press. For the other two tasks, the Stim1 and Stim2 images were composed of a single stimulus without any distracting/overlapping information: a face in the face memory task (FM) and a scene in the scene memory task (SM). The task was presented in 2 separate blocks, each block consisting of all 5 task sets counterbalanced in random order across all participants. Each task set consisted of 30 trials (60 total trials per task, 120 total Encode Period images).

Following the main experiment, participants performed a surprise post-experiment recognition test in which they viewed 320 non-overlapped images, including 160 faces and 160 scenes. 80 of the faces and 80 of the scenes were novel stimuli that were not included in the main experiment. There were 20 faces each from the FM, FM-O, SM-O, and PV-O tasks, and 20 scenes each from the SM, SM-O, FM-O, and PV-O tasks. No stimuli in the post-experiment test were seen more than once before. All included face and scene stimuli (both novel images and images from the experiment) were randomly ordered, and participants were asked to rate their recognition of each image on a scale from 1- 4. For analysis of this data, each participant's ratings were collapsed across stimulus type and normalized to their average rating for novel stimuli. Scores were then collapsed across conditions and broken into the following categories: No-Overlap (stimuli from the SM and FM conditions), Overlap-Relevant (scenes and faces from the SM-O and FM-O conditions, respectively), Overlap-Irrelevant (faces and scenes from the SM-O and FM-O conditions, respectively), and Passive-View (faces and scenes from the PV-O condition).

Stimuli. All stimuli consists of 225x300 pixel grayscale images, presented foveally, subtending a visual angle of 3° from a small cross at the center of the image. The face stimuli consisted of a variety of neutral-expression male and female faces across a large age range. Hair and ears were removed digitally, and a blur was applied along the contours of the face as to remove any potential non-face-specific cues. The gender of the face stimuli was held constant within each trial. Images of scenes were not digitally modified beyond resizing and grayscaling. For the tasks consisting of overlapped faces and scenes, one face and one scene were randomly paired, made transparent, and

digitally overlapped using Adobe Photoshop CS2 such that both were equally visible. Overlapped and isolated images were randomly assigned to the different tasks.

Localizer and Default Network. To identify visual association cortex (VAC) regions maximally responsive to scenes and faces (the parahippocampal place area – or PPA – and the face fusiform area – or FFA, a localizer task independent of the main experimental task was performed, which consisted of 14 interleaved, 12 sec blocks of 20 scenes or faces with a 8 sec delay between each block [2, 3]. To ensure participant's maintained vigilance, they were asked to press a button whenever they saw the exact same stimulus presented twice in a row (10% of stimuli presented). fMRI data was acquired and processed as described below. A contrast was created from the general linear model (GLM) ß-maps for scenes and faces and the most active 35 voxels (~0.390 cm^3) were selected from the approximate anatomical location for each of the following: left PPA (lPPA), right PPA (rPPA), left FFA (lFFA), and right FFA (rFFA) [2]. Default network activity was functionally defined as regions where there was greater degree of activity during rest compared to 1-back [4]. ROIs for the default network were defined using clusters of activity anatomically constrained to published coordinates of network nodes [5].*

fMRI Collection and Processing. All fMRI data were collected on a Siemens 3T MAGNETOM Treo 3T scanner with stimuli presented on an LCD monitor viewed in the prone position by participants using a mirror rigidly attached to the 12-channel head-coil. Echoplanar imaging (EPI) data was acquired (FA=90, TE = 25 ms, TR = 2 sec) with 33 interleaved axial slices (with a 0.5mm gap) for a final resolution of 1.79x1.79x3.5mm/voxel (FOV = 23 cm; 128x128 matrix). All data preprocessing was conducted in SPM5 (Wellcome Department of Imaging Neuroscience, London, England). Raw blood oxygen level dependent (BOLD) data was corrected offline for slice-timing acquisition and motion-artifacts. A 5mm isotropic Gaussian smoothing kernel was applied using SPM5 prior to modeling the data. In addition to the EPI data, high-resolution T1-MPRAGE images (1 x 1 x 1 mm voxel size; FOV = 160 x 240 x 256 mm,

* It should be noted, that the default network was generated via univariate analysis, which technically does not reveal a "network". However, the same set of default regions have also been shown via functional connectivity analysis during a period of a rest[24]

TR = 2300 ms, TE = 3 ms, FA = 90) were acquired to aid in anatomical localizations of activity and to screen for any undiagnosed neurological trauma.

Region of interest (ROI) activities were calculated by modeling the encoding (including both stimuli and the ISI), delay periods, and probe periods in each condition using a boxcar function convolved with the canonical hemodynamic response function (HRF) for the duration of each epoch as a general linear model (GLM) within SPM5. Native-space masks for each posterior ROI were created for each participant as described above and the estimated coefficients for encode-period activity were used as a measure of posterior VAC activations. Group-level univariate analysis was performed by normalizing each participant's mean EPI image to the Montreal Neurological Institute (MNI; 2 x 2 x 2 mm voxel size) template image prior to Gaussian smoothing and modeling.

Network Analysis. Functional connectivity network maps were created for each participant as described previously using a beta-series correlation analysis approach [6, 7]. The encode, delay and probe stage from each condition and every trial was modeled with its own distinct regressor within the GLM, although only the encode period activity was analyzed below. The average value was extracted for each VAC ROI for each trial and these values were then correlated voxel-wise across the entire brain to find regions with highly revealed regions with co-varying activity across trials with the VAC-ROI. The whole-brain r value maps for each participant underwent a Fisher's r to z transformation and the z-values were then normalized to the MNI-template and Gaussian smoothed (5 mm FWHM) for group level analysis. Group contrast maps were created by permuting across the condition grouping term and averaging across the group using 10000 rounds of permutation [8]. Data was corrected for multiple comparisons by thresholding the p-values at 0.05 and permuting across the expected cluster distribution to find the expected cluster size for p = 0.05. Clusters smaller than this value were removed from the analysis [8].

Whole-Brain Neural-Functional Connectivity Correlations: Correlations between each participant's index of suppression (encode period values for the PPA: the difference between the FM-O and PV-O conditions) and the degree of functional connectivity between the PPA and every other voxel were performed on MNI-normalized

images, thresholded at $p < 0.05$ and corrected for multiple comparisons using the permutation method described in the Network Analysis section above.

Whole-Brain Reaction Time Correlations with Activity. Using the beta-series approach as described above, RT data was correlated with trial-by-trial variations in the modeled BOLD signal for every voxel in the brain for each participant. A Fisher's r to z transformation was applied and followed by t-tests to determine regions exhibiting significant correlations at the group level independently for both the main-effects of the overlapped condition (FM-O) and the non-overlapping condition (FM). To determine which regions were correlated significantly different between the overlapped and non-overlapped conditions, a contrast of Z-values was created (FM-O – FM) and significance was determined using 10000 rounds of a permutation test (described above). Both main-effects and contrast images were thresholded at $p < 0.05$ and corrected for multiple comparisons using the permutation method described in the Network Analysis section above.

Whole-Brain Behavioral-Functional Connectivity Correlations. A behavioral index was created for each participant using the difference in RTs for the overlapped condition (FM-O) and the non-overlapped condition (FM) to normalize participants' performance by bottom-up sensory processing. Each participant's behavioral index was correlated on a voxel-by-voxel basis with a functional connectivity index composed of the difference in PPA connectivity in the overlapped (FM-O) and non-overlapped conditions (FM). This analysis was performed on MNI-normalized images, thresholded at $p < 0.05$ and corrected for multiple comparisons using the permutation method described in the Network Analysis section above[1]. This same analysis was also performed using the FFA as a seed regions and SM-O and SM as the conditions.

Comparative Statistics. ANOVA's were utilized throughout analysis. Post-hoc two-tailed t-tests were corrected for multiple comparisons using Tukey-Kramer's method.

SUPPLEMENTARY RESULTS

Behavioral Performance. WM accuracy and response time (RT) data were subjected to separate repeated-measures 2x2 analysis of variance (ANOVA) with type of stimuli attended (face vs. scene) and overlap status (overlapped vs. non-overlapped) as factors (**Fig. 1**). WM accuracy analysis revealed a main effect of overlap ($F_{1,21} = 70.1$; $p < 0.0001$), such that accuracy was significantly reduced in tasks with overlapped stimuli relative to tasks with face and scene stimuli presented in isolation (Face-Memory-Overlap: FM-O—79.4% vs. Face-Memory: FM—88.6%, $p < 5x10^{-7}$; Scene-Memory-Overlap: SM-O—78.3% vs. Scene-Memory: SM—92.6%, $p < 1x10^{-12}$) (**Supplementary Fig. 1a**). This WM performance reduction for the overlapping stimuli was also evident as an increased RT for the overlap tasks ($F_{1,21} = 28.4$; $p < 0.0001$), (FM-O— 1323 ms vs. FM—1197 ms, $p < 0.0019$; SM-O—1144 ms vs. SM—1303 ms, $p < 0.001$) (**Supplementary Fig. 1b**). This supports previous findings that overlapped stimuli involve conflicting information that reduces WM performance [1]. There was also a main effect of type of stimulus attended for WM accuracy ($F_{1,21}=4.8$; $p < 0.05$), but no interaction between stimulus type and overlap ($F_{1,21}=1.17$; $p < 0.287$). Post-hoc comparisons revealed that accuracy was reduced for faces compared to scenes, but only in the non-overlapped tasks (SM—92.6%, FM—88.6%, $p < 0.01$). There was no main effect of stimulus for RT, and no interaction between stimulus and overlap for RT. Accuracy in the passive view (PV-O) task was 99.1%; reaction times to arrow direction averaged 697 ms.

In addition to measures of WM performance, participants also performed a post-experiment evaluation of long-term memory (**Supplementary Fig. 1c**). Participants had higher long-term retention of stimuli from the non-overlapped conditions (FM and SM) compared to the overlapped conditions (FM-O, SM-O, and PV-O, $p<0.005$). In addition, for overlapped stimuli, participants remembered task-relevant stimuli significantly better than task-irrelevant stimuli (e.g., faces in the FM-O > scenes in FM-O, $p<0.05$).

Univariate data: Stimulus-selective, visual association cortex areas. Neural measures of top-down modulation in visual cortices were derived by modeling encoding-period activity using a GLM and extracting beta values associated with activations from the left PPA and right FFA , as previous studies show these are the most robust regions of face and scene selective activity modulation [2, 9, 10]. Data from the PPA revealed the

expected bottom-up scene-selectivity of this region, such that stimuli that include scenes alone (SM) demonstrated significantly greater responses than stimuli with faces alone (FM) (**Supplementary Fig. 2a**). In addition, there was a significant top-down modulation effect, such that all three overlapped conditions revealed significantly different patterns of activation depending on the goals of the task: enhancement of PPA activity when scenes were relevant compared to passive-view baseline (SM-O > PV-O; $p<0.001$), and significant suppression of PPA activity when scenes were irrelevant compared to baseline (FM-O < PV-O; $p<0.005$), consistent with the ROI results using a similar paradigm with sequential presentation of faces and scenes [2]. These three levels of activation (SM-O > PV-O > FM-O) represent a pure, top-down effect because bottom-up information was constant across tasks. In addition, the magnitude of the ROI effects for the overlapped conditions fell between the levels attained in pure conditions (SM > SM-O > PV-O > FM-O > FM). A similar pattern of activation was observed for the FFA (**Supplementary Fig. 2b**). A significant bottom-up effect was demonstrated, such that FM > SM, as well as significant enhancement (FM-O > PV-O). However, there was not a robust measure of suppression within the FFA (SM-O < PV-O), consistent with a previous finding investigating enhancement and suppression within the VAC [2].

Whole-Brain functional connectivity. Capitalizing on trial-by-trial variability, whole-brain functional connectivity maps were assessed by correlating activity from the VAC ROIs (seed regions) with voxels from the rest of the brain [6, 7]. Regions that are highly correlated with a VAC seed across trials are presumed to be functionally connected, thereby defining large-scale networks associated with activity modulation that occurs in those regions. By differentially pairing a seed with a task condition, enhancement and suppression networks can be evaluated. An “enhancement network” map was generated by contrasting PPA connectivity maps obtained during SM-O with those during PV-O (i.e., comparing the PPA network map during the condition when scenes were behaviorally relevant, to the network from the condition when there were no attentional demands. Note: the same stimuli and seed regions were used, just the pairing of seed and condition differed) [9]. Comparably, a “suppression network” map was generated by contrasting the PPA connectivity maps obtained in the FM-O and PV-O contrast (i.e., comparing the condition when scenes were behaviorally irrelevant, to the condition when there were no attentional demands). Brain regions more strongly correlated with the PPA

in SM-O and FM-O compared to PV-O are potentially associated with enhancement and suppression processes, respectively. The same analysis was performed using the FFA as a seed region and differentially pairing it with conditions to yield enhancement and suppression networks. Note that these analyses are correlational and do not reveal that enhancement and suppression network regions are sources of top-down control, but rather that they are associated with VAC regions that are enhanced or suppressed.

Analysis of the whole-brain enhancement networks demonstrated that visual cortical ROIs representing relevant information were functionally connected with regions that have been previously defined as the frontal-parietal network (FPN) [5, 11]: the right middle frontal gyrus (MFG), bilateral inferior frontal junction (IFJ,) superior intraparietal sulcus (sIPS), and supplementary motor area (SMA) (**Fig. 2a, b; Supplementary Table 1**). Interestingly, the enhancement network using the PPA seed (**Fig. 2a**) involved similar regions as the enhancement network using the FFA seed (**Fig. 2b**). This suggests that comparable frontal and parietal regions are associated with enhancement of task-relevant visual stimuli regardless of stimulus type, consistent with these regions being involved in a diverse array of attentionally demanding tasks [9, 11-13].

Analysis of the suppression network revealed a different set of regions from those identified in the enhancement network. Specifically, regions in the medial prefrontal cortex (mPFC), posterior cingulated cortex (PCC), retrosplenial cortex (ReSp), and bilateral parietal cortex (PC) were functionally coupled with visual cortical seeds representing the irrelevant stimuli (**Fig. 2c, d; Supplementary Table 2**). Notably, these brain regions are key nodes of the default network (DN) [5, 14]. As with the enhancement network, the suppression network was observed to be largely independent of seed region (PPA – **Fig. 2c** and FFA – **Fig. 2d**), despite the FFA not achieving significant suppression.

Direct Comparison of the Suppression Network and Enhancement Network. To evaluate which regions were unique to the enhancement or suppression networks, we directly contrasted the enhancement and suppression networks (**Fig. 2e, f; Supplementary Table 3**). This analysis revealed distinct networks and highlighted regions specific to the enhancement network, notably the right MFG, left IFJ, and right IFJ (**Fig. 2e, f**: blue colors; labeled 1, 2, and 3, respectively), and regions specific to the

suppression network, notably DN regions. The mPFC and PCC (**Fig. 2e, f**: red colors; labeled 4, and 5, respectively), as well as a large region of the left lateral parietal cortex.

Comparison of the Suppression Network and the Default Network.

To explore the relationship between the suppression network and the DN, a whole-brain conjunction analysis was performed in which voxels were identified that showed both significant suppression network connectivity and DN activity corrected for cluster size (**Supplementary Fig. 3, Supplementary Methods**). The suppression networks were assessed using both PPA and FFA seeds. The DN was identified using the independent localizer task and contrasting rest > task blocks (**Supplementary Fig. 3a, b**, first rows), which yielded the canonical DN [5, 14]. Strikingly, the conjunction analysis revealed that there was a high degree of overlap between the suppression networks and the medial regions of the DN, most notably the PCC and mPFC. (**Supplementary Fig. 3a, b**, bottom rows (magenta)).

We further explored this relationship by using DN ROIs identified by the independent localizer. Consistent with our previous observations, we demonstrated greater functional connectivity between visual cortical regions and DN regions when the information represented by stimulus-selective visual regions was irrelevant to the participant's goals, compared to when the information was relevant (notably, mPFC, and PCC) (**Supplementary Fig. 4**). For example, the PPA exhibited greater connectivity with mPFC and PCC during the condition when scenes were irrelevant (FM-O), than the condition when scenes were relevant (SM-O). This pattern was consistent for the same stimuli using a different seed region, such that the FFA demonstrated greater connectivity with the mPFC and PCC in the condition when scenes were irrelevant (SM-O), than the condition when faces were relevant (FM-O). Moreover, analysis revealed that differential connectivity of stimulus-selective visual regions with DN regions occurred simultaneously, such that differential connectivity was present during each condition. For example, during FM-O, there was greater connectivity between the mPFC and PPA than with FFA, a pattern that was reversed with the same stimuli but when task goals were switched (i.e., during SM-O, there was greater connectivity between the mPFC and FFA than with PPA) (**Supplementary Fig. 5**, middle panels). Interestingly, this phenomenon required the presence of irrelevant information. In conditions without task-irrelevant information present (i.e., FM and SM), but with the same goals as when stimuli

contained irrelevant information (i.e., FM-O and SM-O), neither the PPA nor the FFA were significantly connected with DN regions (**Supplementary Fig. 5**, outer panels). Thus, the suppression network depicted in **Fig. 2c, d** are generated based on task goals, but requires the presence of conflicting, irrelevant information.

Because of the correlational nature of the network measure, there is the possibility that the DN/VAC relationship may not exist in the non-overlap condition because of less signal variance in the contributing regions. Analysis of the standard deviation of the BOLD signal across trials within each participant and then evaluated at the group level revealed that neither the mPFC nor the PPA showed significant differences in the signal variance between the overlapped and non-overlapped conditions (mPFC: 0.7605 and 1.0142, respectively: t-test, p=0.4799; PPA: 1.7510 and 1.8433, respectively: t-test, p=0.7541). This suggests that the lack of coupling in the non-overlapped conditions compared to the overlapped condition is evidence that the relationship between DN and sensory regions reflects a more complex interaction, one dependent on the presence of irrelevant information.

Suppression Network vs. Visual Cortical Activity Suppression. To further explore the relationship between VAC activity modulation and network connectivity, we performed across-participant, whole-brain regression analyses. While we did not find connectivity with any FPN regions that served as significant predictors of the magnitude of activity enhancement, the magnitude of PPA suppression was predicted by the degree of functional connectivity between the PPA and the mPFC (**Supplementary Fig. 6**), such that participants with stronger coupling between the PPA and mPFC showed greater suppression of activity associated with task-irrelevant scenes. This effect was limited to PPA, consistent with the univariate ROI results that revealed PPA exhibited more robust suppression than FFA (**Supplementary Fig. 2**).

Reaction-time data vs. Whole-brain activity. We performed a regression analysis of trial-by-trial response times (RTs) and BOLD signal across every voxel in the brain for each participant. On the group level, we demonstrated that trial-by-trial activity fluctuations within DN regions were significantly correlated with RT (particularly the mPFC and PCC; corrected for multiple comparisons) in the overlapped conditions, such that trials that exhibited the greatest suppression of activity in DN regions during

stimulus presentation were those trials that exhibited the fastest RT at probe (high performance) (**Supplementary Fig. 7a**). When the RT-activity correlation was performed on those conditions without overlapping stimuli, there was no significant correlation (**Supplementary Fig. 7b**). When overlapped vs. non-overlapped correlations were directly compared, we demonstrate that the correlation was significantly greater in the overlapped vs. non-overlapped conditions (**Supplementary Fig. 7c**). This neural-behavioral finding is comparable to the results showing that significant DN coupling with visual areas occurs only when task-irrelevant stimuli are present.

Relationshp between RT and VAC connectivity. We performed an across-participant regression analysis between the impact of irrelevant information on behavioral performance (RT for overlapped condition minus RT for non-overlap condition (FM-O minus FM)) and the impact of irrelevant information on functional coupling between the PPA and the rest of the brain (FM-O minus FM). This demonstrated a strong and significant negative correlation between RT and PPA-mPFC functional connectivity, a component of the DN (corrected for multiple comparisons). This data revealed that those participants who exhibited stronger coupling between mPFC and PPA when task-irrelevant information was present, versus when it was absent (i.e., larger difference between FM-O and FM), better preserved their performance when irrelevant information was present, compared to when it was absent (i.e., smaller difference between FM-O and FM) (**Supplementary Fig. 8)**. Of note, this same relationship was not significant when the FFA was the seed region and SM-O and SM were the conditions, consistent with the lack of significant suppression in the FFA.

.

SUPPLEMENTARY DISCUSSION

The data presented provides the first direct evidence that sensory cortex is differentially associated with defined functional networks based on task goals. When visual cortex is associated with behaviorally relevant stimuli (i.e. they are to be actively remembered), we demonstrated both that visual cortex shows an *increased* neural response to the stimuli relative to a passive viewing condition (enhancement) *and* that it is functionally correlated with activity in the FPN. Conversely, when sensory input is to be actively ignored, sensory cortex shows a *decreased* neural response relative to passive viewing (suppression) and is functionally coupled with the DN. Interestingly, both these modulatory/network-association processes occur simultaneously and switch based on task goals, independent of stimulus type. These results present a novel association between sensory cortex and putative frontal and parietal top-down control regions.

The enhancement network corresponds closely to a network shown to be associated with attentional and executive processes. This network, largely revealed via univariate analysis, has been referred to by various terms, including the FPN, dorsal-attention network and the task-positive network [4, 5, 11, 15], although the general set of regions is consistent across naming schemes. A proposed role of these dorsal frontal and parietal regions is that they are the source of top-down modulatory influences on sensory cortical activity, such that they provide direct, long-range signaling to sensory areas to enhance activity based on task goals [16]. This is supported by functional neurophysiological studies in experimental animals [17-19]. Our interpretation of the robust functional connectivity between enhanced VAC regions and this network is that these areas are sources of top-down control (**Supplementary Table 1**). This conclusion is also supported by our previous study using fMRI connectivity analysis and *sequential*, rather than *simultaneous* stimulus presentation [9].

It is important to note that fMRI approaches are correlational in nature and are unable to be used to make strong statements of causality. Another approach would be to utilize a recording technique with high temporal resolution (such as EEG) to investigate the timing of distal communication (for example, do both the FPN and the DN act in an anticipatory fashion prior to stimulus onset as a mechanism for “priming” VAC regions based on task-goals or is there real-time communication that allows efficient processing of stimuli within selective VAC regions). However, EEG is also correlational and so to truly establish causality in demonstrating that area A is communicating with

area B, the system would have to be carefully perturbed in a controlled fashion using a technique such as transcranial magnetic stimulation, and coupled with a recording technique. Since our results indicate that separate networks are differentially involved in the processes of enhancement and suppression, one could perturb a node differentially involved in either enhancement or suppression to prove causality by showing that you selectively disrupt the neural signature of enhancement or suppression.

Suppression of activity within DN regions has been observed during goal-directed behavior [4, 20-23]. Here we extend these findings by showing that trial-by-trial fluctuations in activity within DN regions, notably the mPFC, covaries with activity fluctuations of VAC representing irrelevant, external information. Given the overlap between the suppression network and the DN (**Supplementary Fig. 3**), it is reasonable to speculate that DN regions are a direct source of VAC activity suppression. However, if DN regions were a source of suppressive influence, one might expect there to be a negative correlation. That is, if on a given trial VAC activity was reduced, then activity in frontal and parietal regions of the suppression network serving as the source of such modulation might be expected to be elevated. Instead we find a positive correlation, such that reduced VAC activity is linked with lower activity in DN regions.

Recent evidence suggests that the DN is related to introspective or internalized cognitive processes, such as mind-wandering [24, 25]), and retrospective and prospective memory [14, 25]. Activity in DN regions, notably the mPFC [26], are increased during these internal processes [24, 25, 27], while they are suppressed during tasks that are directed at external events [4, 20-23], presumably as a means of reducing internal distraction. In fact, the degree of deactivation and fidelity of this collective network is predictive of performance [21, 28]. Based on this literature, our interpretion of the overlap between the suppression network and the DN is that it reflects a coupling across trials of suppression of irrelevant external information and suppression of internal activities, both of which if not suppressed would conflict with achieving the goals of the task. This link suggests that a common mode of suppression of task-irrelevant information is engaged regardless if our internal or external environment presents a conflict with task goals. One of the most intriguing aspects of our results is that the degree of activity suppression in the PPA correlated with the degree of connectivity between the PPA and the mPFC during the act of scene suppression. This implies that there may be a facilitatory aspect of the

coupling between these two acts of suppression. In addition, there was a significant relationship between the degree of coupling and WM performance across participants.

The finding in this study of functional connectivity between the suppression network and DN is in direct contrast to results reported previously using a simultaneous presentation version of this task, which revealed a topographically overlapping FPN for enhancement and suppression, with reduced connectivity during suppression [9]. It is possible that the disparity may reflect differences in the demands of the two tasks, since DN deactivation has been shown to be modulated by cognitive load [29], such that increased load results in greater deactivation. However, since the results were not quantitatively, but qualitatively different, it raises interesting questions regarding the nature of conflict and the neural systems utilized when resolving conflict. In the current study, there was direct competition for visual processing recourses, while in the sequential version of the task the competition was indirect, and presumably between new information and information maintained in WM. The combined data suggest that ignoring irrelevant information encountered in isolation involves diminished connectivity between visual regions and FPN, while when irrelevant information is in direct conflict with ongoing sensory processing it involves coupling visual regions with the DN. In support of this finding, the results of the current study revealed that the coupling of suppressed VAC regions and the DN only existed in the presence of conflicting task-irrelevant information

The overlap between of the suppression network and the DN may elucidate findings that normal aging is associated with both a deficit in suppressing external irrelevant information [3, 30, 31] and a decreased ability to deactivate the DN during tasks [4, 14, 21, 22, 32]. This may represent further evidence of a relationship between these networks and a possible mechanistic basis to account for age-related suppression deficits. Functional imaging studies in older adults will be important in examining the relationship between suppression of distraction from both the internal and external environment.

SUPPLEMENTARY FIGURE LEGENDS

Supplementary Figure 1: Behavioral Results. A. Accuracy comparisons for participants across all conditions (n=22). There is an effect of performance on overlapped images (FM-O and SM-O) compared to non-overlapped images (FM and SM), but no effect of stimulus type (FM-O vs. SM-O and FM vs. SM). B. Reaction-time comparisons. Similar results as in A. C. Long-term memory scores. Participants remembered stimuli with no overlap significantly better than those with overlap ($p<0.005$). In the overlapped conditions, task-relevant images were retained better than task-irrelevant images ($p<0.05$). Black colors represent no distractor, grey – distractors, white –passive-view. Error-bars represent S.E.M.

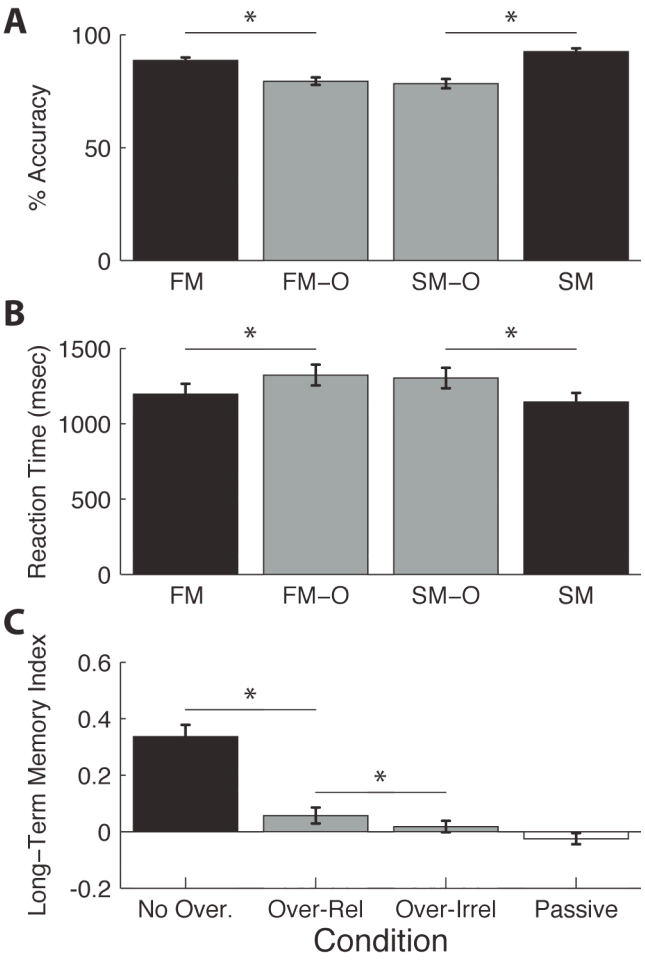

Supplementary Figure 2: Encoding period activity for visual association cortex regions of interest. A. Parameter estimates for a scene-selective region (parahippocampal place area: PPA) are significantly different between each condition, with the difference between SM-O and PV-O reflecting enhancement and the difference between PV-O and FM-O reflecting suppression. B. Same as A, but using the face-selective region (face fusiform area: FFA) (*p<0.05). Error-bars represent S.E.M.

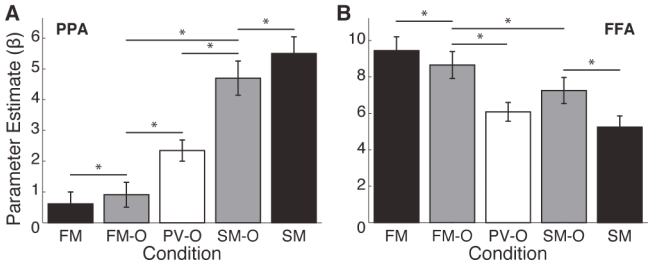

Supplementary Figure 3: Comparisons between the default-network and suppression network for PPA (A) and FFA (B). Whole-brain maps were cluster corrected for multiple comparisons at p=0.05 and displayed at p=0.01. Note that the first row in both A and B are the same images and are only repeated to allow ease of visual comparisons. Same numbered labels as in Figure 3.

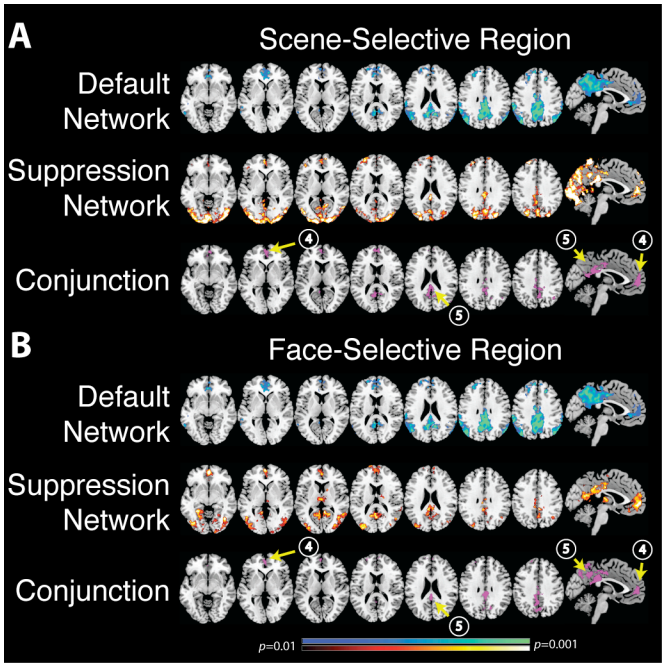

Supplementary Figure 4: Extracted functional connectivity data for visual association cortex (FFA and PPA) – default-network regions of interest, comparing between the remember faces (FM-O) and remember scenes (SM-O) conditions. White bars represent connectivity values during enhancement and black bars during suppression (*p<0.05). Error-bars represent S.E.M.

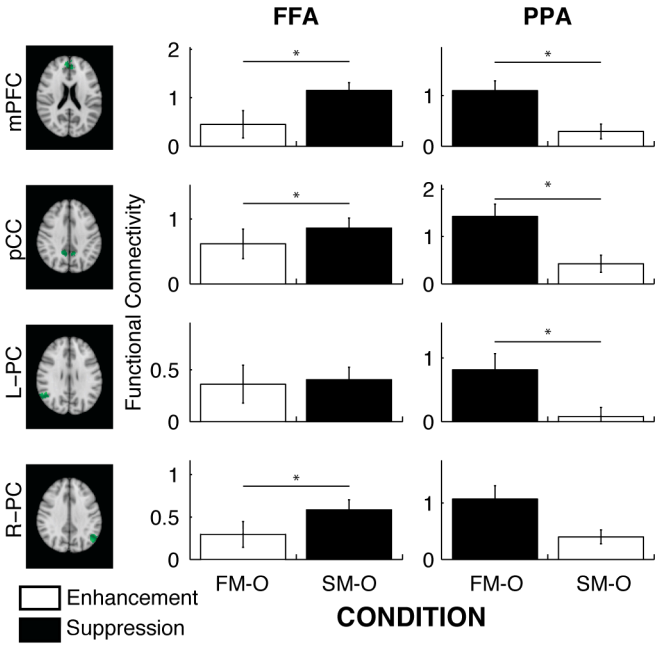

Supplementary Figure 5: Functional connectivity maps focusing on mPFC connectivity with different VAC seeds across conditions. Inner panels, upper vs. lower reveals selective connectivity of VAC regions and mPFC only in the suppression network. However, this mPFC connectivity only occurs when irrelevant information is present in the image (compare outer panels). Same numbered labels as in Figure 3.

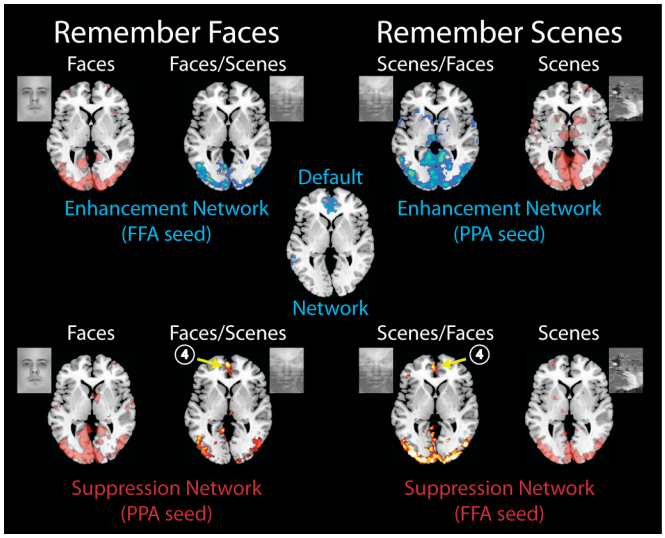

Supplementary Figure 6: Group-data of a voxel-wise regression between the magnitude of PPA suppression (PV-O – FM-O) and PPA functional connectivity (FM-O – PV-O) showing a significant correlation in the mPFC ($p<0.05$ for Pearson's correlation corrected for multiple comparisons, see methods). Same numbered labels as in Fig. 2.

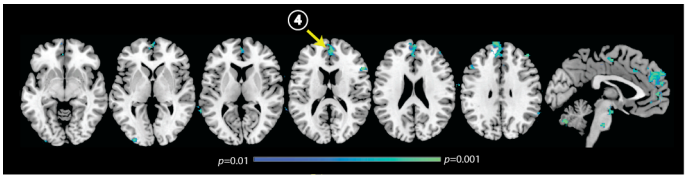

Supplementary Figure 7: Trial-by-trial correlation between reaction time and whole-brain activity. A. Whole-brain correlation between RT data and activity during the FM-O condition. B. Whole-brain correlation between RT data and activity during the FM condition (non-overlapped images, no irrelevant information present). C. Contrast of A vs. B showing that activity in default mode regions was only correlated with RT when task-irrelevant information was present. Images displayed at $p<0.05$ with cluster correction (see Methods).

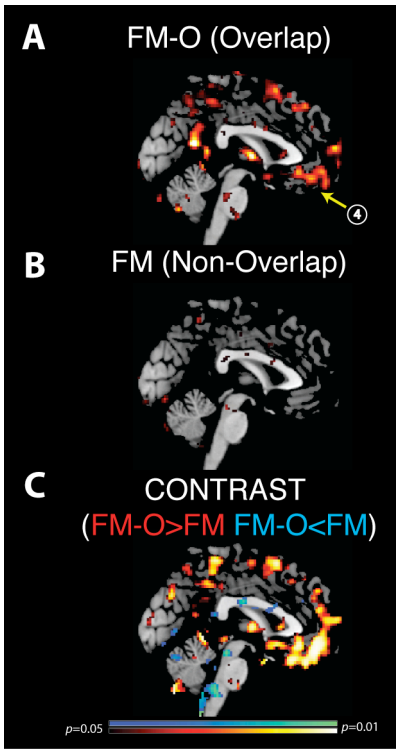

Supplementary Figure 8: Whole-brain correlation between the impact of distraction on RT (FM-O – FM) and the impact of distraction on functional connectivity with the VAC (FM-O – FM). There was a strong negative correlation (red) between DN-PPA connectivity and the RT measure suggesting that greater VAC-DN functional connectivity is associated with better behavioral performance the setting of distracting information. No significant positive correlations (blue) were observed ($p<0.05$).

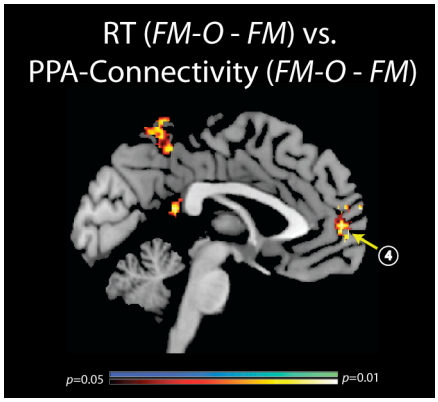

SUPPLEMENTARY TABLES

Supplementary Table 1: Enhancement Network. Regions that exhibit significantly greater functional connectivity for Remember > Passively View for scenes (PPA: SMO > PVO) and faces (FFA: FMO > PVO). Significance was determined as described in methods: whole-brain images were thresholded at $p<0.05$ using FDR and cluster correction. Coordinates are in MNI space.

PPA Enhancement (SMO>PVO)

NAME	X	Y	Z
right Middle Frontal Gyrus (rMFG)	34	50	24
left Middle Frontal Gyrus (lMFG)	-34	46	32
left Inferior Frontal Junction (lIFJ)	-54	12	34
right Inferior Frontal Junction (rIFJ)	50	10	34
Supplementary Motor Area (SMA)	2	2	58
right Superior Parietal Lobule (rSPL)	30	-58	56

FFA Enhancement (FMO>PVO)

NAME	X	Y	Z
right Middle Frontal Gyrus (rMFG)	38	44	36
right Inferior Frontal Junction (rIFJ)	48	12	34
left Inferior Frontal Junction (lIFJ)	-48	2	32
Supplementary Motor Area (SMA)	0	2	46
right Frontal Eye Fields (rFEF)	48	-12	48
left Frontal Eye Fields (lFEF)	-46	-12	46
right Superior Parietal Lobule (rSPL)	44	-48	56
left Superior Parietal Lobule (lSPL)	-40	-48	54

Supplementary Table 2: Suppression Network. Regions that exhibit significantly greater functional connectivity for the Ignore > Passively view for scenes (PPA: FMO > PVO) and faces (FFA: SMO > PVO). Significance was determined as in Table 1. Coordinates are in MNI space.

PPA Suppression (FMO>PVO)

NAME	X	Y	Z
medial Prefrontal Cortex (mPFC)	2	56	-6
Posterior Cingulate Cortex (PCC)	2	-40	34
Retrospinial Cortex (reSp)	-4	-58	16
right Angular Gyrus (rAngG)	40	-64	40

FFA Suppression (SMO>PVO)

NAME	X	Y	Z
medial Prefrontal Cortex (mPFC)	-4	52	2
left Frontal Pole (lFP)	-32	50	30
left Middle Frontal Gyrus (lMFG)	-42	42	10
Posterior Cingulate Cortex (PCC)	0	-34	32
left Superior Parietal Lobule (lSPL)	24	-64	60

Supplementary Table 3: Regions significantly different in a contrast between enhancement and suppression network maps. Significance was determined as in Table S1. Coordinates are in MNI space.

PPA Enhancement > Suppression

NAME	X	Y	Z
right Middle Frontal Gyrus (rMFG)	34	54	26
right Inferior Frontal Junction (rIFJ)	54	12	38
left Inferior Frontal Junction (lIFJ)	-56	12	34
Supplementary Motor Area (SMA)	-4	12	46
right Intraparietal Sulcus (rIPS)	36	-44	42
right Angular Gyrus (rAngG)	36	-76	24
left Inferior Parietal Lobule (lIPL)	-38	-84	34

FFA Enhancement > Suppression

NAME	X	Y	Z
right Inferrior Frontal Junction (rIFJ)	40	8	38
right Middle Frontal Gyrus (rMFG)	50	28	32
Supplementary Motor Area (SMA)	0	16	66
right Superior Parietal Lobule (rSPL)	16	-72	60
left Superior Parietal Lobule (lSPL)	-12	-72	58

PPA Suppression > Enhancement

NAME	X	Y	Z
medial Prefrontal Cortex (mPFC)	2	52	0
right Frontal Pole (rFP)	42	38	-16
right Insula (rIN)	44	4	-12
left Insula (lIN)	-42	6	-16
left Superior Frontal Gyrus (rSFG)	-22	30	40
left Inferior Parietal Lobule (lIPL)	-50	-56	36

Posterior Cingulate Cortex (PCC)	6	-52	34
Retrospinial Cortex	-4	-58	16
right Inferior Temporal Cortex (rITC)	54	-10	-26

FFA Suppression > Enhancement

NAME	X	Y	Z
medial Prefrontal Cortex (mPFC)	-4	52	2
left Frontal Pole (lFP)	-32	50	30
left Temporalparietal Junction (lTPJ)	-54	-32	4
Posterior Cingulate Cortex (PCC)	0	-34	32
left Inferior Parietal Lobule (lIPL)	-48	-68	26

SUPPLEMENTARY REFERENCES

1. Rutman, A.M., Clapp, W.C., Chadick, J. & Gazzaley, A. Early Top-Down Control of Visual Processing Predicts Working Memory Performance. *J Cogn Neurosci* (2009).
2. Gazzaley, A., Cooney, J., McEvoy, K., Knight, R.T. & D'Esposito, M. Top-down enhancement and suppression of the magnitude and speed of neural activity. *J Cogn Neurosci* **17**, 507-517 (2005).
3. Gazzaley, A., Cooney, J., Rissman, J. & D'Esposito, M. Top-down suppression deficit underlies working memory impairment in normal aging. *Nat Neurosci* **8**, 1298-1300 (2005).
4. Grady, C.L., Springer, M.V., Hongwanishkul, D., McIntosh, A.R. & Winocur, G. Age-related changes in brain activity across the adult lifespan. *J Cogn Neurosci* **18**, 227-241 (2006).
5. Fox, M.D.*, et al.* The human brain is intrinsically organized into dynamic, anticorrelated functional networks. *Proc Nat Acad Sci USA* **102**, 9673-9678 (2005).
6. Gazzaley, A., Rissman, J. & D'Esposito, M. Functional connectivity during working memory maintenance. *Cogn Affect Behav Neurosci* **4**, 580-599 (2004).
7. Rissman, J., Gazzaley, A. & D'Esposito, M. Measuring functional connectivity during distinct stages of a cognitive task. *NeuroImage* **23**, 752-763 (2004).
8. Nichols, T.E. & Holmes, A.P. Nonparametric permutation tests for functional neuroimaging: a primer with examples. *Hum Brain Mapp* **15**, 1-25 (2002).
9. Gazzaley, A.*, et al.* Functional interactions between prefrontal and visual association cortex contribute to top-down modulation of visual processing. *Cereb Cortex* **17 Suppl 1**, i125-135 (2007).
10. Rissman, J., Gazzaley, A. & D'Esposito, M. The effect of non-visual working memory load on top-down modulation of visual processing. *Neuropsychologia* **47**, 1637-1646 (2009).
11. Corbetta, M., Patel, G. & Shulman, G.L. The reorienting system of the human brain: from environment to theory of mind. *Neuron* **58**, 306-324 (2008).
12. Capotosto, P., Babiloni, C., Romani, G.L. & Corbetta, M. Frontoparietal cortex controls spatial attention through modulation of anticipatory alpha rhythms. *J Neurosci* **29**, 5863-5872 (2009).
13. Weidner, R., Krummenacher, J., Reimann, B., Müller, H.J. & Fink, G.R. Sources of top-down control in visual search. *J Cogn Neurosci* **21**, 2100-2113 (2009).
14. Buckner, R.L., Andrews-Hanna, J.R. & Schacter, D.L. The brain's default network: anatomy, function, and relevance to disease. *Ann N Y Acad Sci* **1124**, 1-38 (2008).
15. Szczepanski, S.M., Konen, C.S. & Kastner, S. Mechanisms of spatial attention control in frontal and parietal cortex. *J Neurosci* **30**, 148-160 (2010).
16. Corbetta, M. Frontoparietal cortical networks for directing attention and the eye to visual locations: identical, independent, or overlapping neural systems? *Proc Nat Acad Sci USA* **95**, 831-838 (1998).
17. Fuster, J., Bauer, R. & Jervey, J. Functional interactions between inferotemporal and prefrontal cortex in a cognitive task. *Brain Res* **330**, 299-307 (1985).

18. Moore, T. & Armstrong, K.M. Selective gating of visual signals by microstimulation of frontal cortex. *Nature* **421**, 370-373 (2003).
19. Tomita, H., Ohbayashi, M., Nakahara, K., Hasegawa, I. & Miyashita, Y. Top-down signal from prefrontal cortex in executive control of memory retrieval. *Nature* **401**, 699-703 (1999).
20. Celone, K.A.*, et al.* Alterations in memory networks in mild cognitive impairment and Alzheimer's disease: an independent component analysis. *J Neurosci* **26**, 10222-10231 (2006).
21. Grady, C.L.*, et al.* A Multivariate Analysis of Age-Related Differences in Default Mode and Task-Positive Networks across Multiple Cognitive Domains. *Cereb Cortex* (2009).
22. Lustig, C.*, et al.* Functional deactivations: change with age and dementia of the Alzheimer type. *Proc Nat Acad Sci USA* **100**, 14504-14509 (2003).
23. Persson, J., Lustig, C., Nelson, J.K. & Reuter-Lorenz, P.A. Age differences in deactivation: a link to cognitive control? *J Cogn Neurosci* **19**, 1021-1032 (2007).
24. Buckner, R.L. & Carroll, D.C. Self-projection and the brain. *Trends Cogn Sci* **11**, 49-57 (2007).
25. Mason, M.F.*, et al.* Wandering minds: the default network and stimulus-independent thought. *Science* **315**, 393-395 (2007).
26. Scheeringa, R.*, et al.* Trial-by-trial coupling between EEG and BOLD identifies networks related to alpha and theta EEG power increases during working memory maintenance. *NeuroImage* **44**, 1224-1238 (2009).
27. Gusnard, D.A., Akbudak, E., Shulman, G.L. & Raichle, M.E. Medial prefrontal cortex and self-referential mental activity: relation to a default mode of brain function. *Proc Nat Acad Sci USA* **98**, 4259-4264 (2001).
28. Andrews-Hanna, J.R.*, et al.* Disruption of large-scale brain systems in advanced aging. *Neuron* **56**, 924-935 (2007).
29. Persson, J., Welsh, K.M., Jonides, J.J. & Reuter-Lorenz, P.A. Cognitive fatigue of executive processes: interaction between interference resolution tasks. *Neuropsychologia* **45**, 1571-1579 (2007).
30. Gazzaley, A.*, et al.* Age-related top-down suppression deficit in the early stages of cortical visual memory processing. *Proc Nat Acad Sci USA* **105**, 13122-13126 (2008).
31. Gazzaley, A. & D'Esposito, M. Top-down modulation and normal aging. *Ann N Y Acad Sci* **1097**, 67-83 (2007).
32. Hedden, T.*, et al.* Disruption of functional connectivity in clinically normal older adults harboring amyloid burden. *J Neurosci* **29**, 12686-12694 (2009).